

Anatomy of Non-Leptonic Two-Body Decays of Charmed Mesons into Final States with η'

Carolina Bolognani^{a,b} Ulrich Nierste^c Stefan Schacht^d K. Keri Vos^{a,b}

^a*Gravitational Waves and Fundamental Physics (GWFP), Maastricht University, Duboisdomein 30, NL-6229 GT Maastricht, the Netherlands*

^b*Nikhef, Science Park 105, NL-1098 XG Amsterdam, the Netherlands*

^c*Institute for Theoretical Particle Physics, Karlsruhe Institute of Technology (KIT), Wolfgang-Gaede-Str. 1, 76131 Karlsruhe, Germany*

^d*Department of Physics and Astronomy, University of Manchester, Manchester M13 9PL, United Kingdom*

E-mail: carolina.bolognani@cern.ch, ulrich.nierste@kit.edu,
stefan.schacht@manchester.ac.uk, k.vos@maastrichtuniversity.nl

ABSTRACT: We show that $D \rightarrow P\eta'$ decay amplitudes, where $P = K, \pi, \eta$, cannot be simply related to their $D \rightarrow P\eta$ counterparts with a single η_0 - η_8 mixing angle. Proposing a novel, consistent treatment of η_0 - η_8 mixing, we perform a global analysis of $D \rightarrow P\eta'$ decays employing $SU(3)_F$ symmetry including linear $SU(3)_F$ breaking. We find that the assumption of 30% $SU(3)_F$ breaking is in slight tension (2.5σ) with the data when compared to a fit that allows for 50% $SU(3)_F$ breaking, the latter giving a perfect description of the data. In order to allow for further scrutinization of $SU(3)_F$ -breaking effects in the future, we give branching ratio predictions for all $D \rightarrow P\eta'$ modes. Our predictions deviate from the current data in case of the branching ratios $\mathcal{B}(D_s^+ \rightarrow K^+\eta')$ and $\mathcal{B}(D^+ \rightarrow K^+\eta')$. Future more precise measurements of these channels are therefore highly important in order to clarify the quality of the $SU(3)_F$ expansion in nonleptonic $D \rightarrow P\eta'$ decays.

Contents

1	Introduction	1
2	Description of D meson decay matrix elements involving $\eta_{0,8}$	3
3	$SU(3)_F$ Decomposition of $D \rightarrow P\eta'$ decays	4
3.1	Topological Decomposition	4
3.2	Linear $SU(3)_F$ -breaking	6
4	Numerical Results	8
4.1	Constraining diagrammatic $SU(3)_F$ breaking	8
4.2	Fit setup and $SU(3)_F$ test	8
4.3	Implications for branching ratios	11
4.4	Theory correlations between branching ratios	12
5	Conclusions	13
A	Notation	15
B	$SU(3)_F$-breaking topological diagrams and decomposition without redefinitions	16

1 Introduction

Charm decays are a laboratory for the exploration of flavor violation in the up quark sector, complementary to the kaon and b physics program. The first evidence of non-zero CP asymmetries in $D \rightarrow \pi^+\pi^-$ decays [1, 2] received a lot of attention and pushes the focus toward measurements of CP violation. Recent developments for further searches for CP violation are very promising [3–9], and future prospects are bright [10–12]. In particular, there has also been recent progress in nonleptonic decays to $\eta^{(\prime)}$ states [13–17].

Predicting hadronic D meson decays is notoriously challenging. The most prospective method to study hadronic D meson decay amplitudes employs the approximate $SU(3)_F$ symmetry of QCD [18–46] which relates hadronic amplitudes of different decays to each other. Control of $SU(3)_F$ breaking effects is important in order to obtain sensitivity to physics beyond the Standard Model (BSM) [46–49]. Data on CP asymmetries have no impact on the predictions of branching fractions, because CP asymmetries involve different, highly suppressed CKM elements multiplying hadronic matrix elements which do not enter the branching ratios. The opposite is not true, instead a thorough global analysis of D branching fractions is needed for the prediction of the CP asymmetries. The plethora of data on branching fractions permits the inclusion of $SU(3)_F$ breaking into such an analysis [33]

and allows predictions for CP asymmetries which partially include $SU(3)_F$ breaking [34]. In Ref. [33] D decays into two pseudoscalars were studied, but final states with η mesons were not included. In this paper, we focus on $D \rightarrow P\eta'$ decays, with $P = \pi, K$ and η .

In and beyond D meson physics, there are several $SU(3)_F$ studies accommodating η - η' mixing with a universal mixing angle θ describing the rotation of the $SU(3)_F$ eigenstates η_0, η_8 into the mass eigenstates η, η' . However, it is known for a long time that this treatment is inconsistent and gives a poor description of data [50–53]. A consistent treatment, based on properly defined $\eta^{(\prime)}$ decay constant involves two decay constants and two mixing angles [50, 51]. For recent calculations with analytical methods and lattice QCD see Refs. [54] and [55], respectively.

In the context of D decays the shortcomings of the single-mixing angle description can be understood as follows: The matrix element $\langle P\eta_8|H|D\rangle$ of the weak Hamiltonian H with some light pseudoscalar meson P is well-defined and related to other $D \rightarrow PP'$ matrix elements by $SU(3)_F$ symmetry. With

$$|\eta_8\rangle = |\eta\rangle \cos\theta + |\eta'\rangle \sin\theta \quad (1.1)$$

one is led to

$$\langle P\eta_8|H|D\rangle = \cos\theta\langle P\eta|H|D\rangle + \sin\theta\langle P\eta'|H|D\rangle, \quad (1.2)$$

but the description in Eq. (1.2) cannot be rigorous, because the masses of η and η' are very different. These matrix elements are three-point functions which depend on three kinematic invariants, namely the squared masses M_D^2 , M_P^2 , and $M_{\eta^{(\prime)}}^2$ and thus will differ due to $M_\eta \neq M_{\eta'}$. This is different from the mass splittings within the $SU(3)_F$ octet such as $M_K \neq M_\pi$ which are $SU(3)_F$ breaking effects and well accommodated by the hadronic parameters describing $SU(3)_F$ breaking in our set-up. On the other hand, $M_\eta \neq M_{\eta'}$ is unrelated to $SU(3)_F$ breaking and an $\mathcal{O}(1)$ effect in the power counting of $SU(3)_F$ breaking.

We further illustrate this feature with an analogy from perturbation theory: One may try to calculate QCD corrections to the $W^+-u_j-\bar{d}_k$ vertex in the basis of quark flavour eigenstates and then rotate the quarks into mass eigenstates; the CKM matrix is the analogue of the mixing angle θ here. This procedure gives the correct result as long as quark masses are neglected (i.e. in the limit of exact flavour symmetry), while the correct result depends on the masses of the involved quarks. Thus the calculation in the symmetry limit supplemented by CKM rotations does not capture the dependence of the vertex function on the masses and momenta of the loop function.

The purpose of this paper is two-fold: We first explain how D decays into final states with η or η' are treated correctly in $SU(3)_F$ analyses. Then we perform a global analysis of $D \rightarrow P\eta'$ branching ratios, with $D = D^0, D^+, D_s^+$, including linear $SU(3)_F$ breaking to test the quality of $SU(3)_F$ symmetry in these decays and to make predictions for future measurements.

After discussing η_0 - η_8 mixing in the context of D decays in Sec. 2, we give the topological amplitude decomposition for $D \rightarrow P\eta'$ decays in Sec. 3. We present our numerical results of a global fit to current data in Sec. 4, before we conclude in Sec. 5. Several details as well as the topological diagrams are given in the Appendix.

2 Description of D meson decay matrix elements involving $\eta_{0,8}$

We define the octet $|\eta_8\rangle$ and singlet $|\eta_0\rangle$ wave functions in terms of the underlying quark-level wave functions as

$$|\eta_8\rangle = \frac{|u\bar{u}\rangle + |d\bar{d}\rangle - 2|s\bar{s}\rangle}{\sqrt{6}}, \quad (2.1)$$

$$|\eta_0\rangle = \frac{|u\bar{u}\rangle + |d\bar{d}\rangle + |s\bar{s}\rangle}{\sqrt{3}}, \quad (2.2)$$

respectively. $SU(3)_F$ breaking in the strong interaction leads to a hermitian η - η' mass matrix with non-zero off-diagonal elements. After removing unphysical phases this matrix is real and can be diagonalised with the η - η' mixing angle θ introduced in Eq. (1.1). Furthermore,

$$|\eta_0\rangle = -|\eta\rangle \sin\theta + |\eta'\rangle \cos\theta. \quad (2.3)$$

θ is an $SU(3)_F$ -breaking parameter which is not directly related to any observable, because the production mechanism and decay rate of η or η' suffers from $SU(3)$ breaking as well. In the theoretical prediction of any observable θ appears together with other $SU(3)$ -breaking parameters. If one tries to define the η - η' mixing angle through measurable quantities, one encounters the situation that more than one mixing angle [50, 51] is needed for the theoretical description and, of course, the such defined angle cannot be immediately used in other observables.

As mentioned in the introduction, the pitfall of using θ in $SU(3)_F$ analyses are the different masses of η and η' . We may use Eqs. (1.1) and (2.3) to express $|P(p_P)\eta(p_\eta)\rangle$ in terms of $|P(p_P)\eta_{0,8}(p_\eta)\rangle$ and do the same with $|P(p_P)\eta'(p_{\eta'})\rangle$, but the Fock states $|P(p_P)\eta_{0,8}(p_\eta)\rangle$ and $|P(p_P)\eta_{0,8}(p_{\eta'})\rangle$ are different and so are the corresponding D decay matrix elements. We write

$$\langle P\eta | H | D \rangle = \cos\theta \langle P\eta_8 | H | D \rangle - \sin\theta \langle P\eta_0 | H | D \rangle \quad (2.4)$$

$$\langle P\eta' | H | D \rangle = \sin\theta \langle P\eta_8 | H | D \rangle' + \cos\theta \langle P\eta_0 | H | D \rangle', \quad (2.5)$$

where

$$\langle P\eta_8 | H | D \rangle' \neq \langle P\eta_8 | H | D \rangle, \quad (2.6)$$

$$\langle P\eta_0 | H | D \rangle' \neq \langle P\eta_0 | H | D \rangle. \quad (2.7)$$

We emphasize that Eqs. (2.4) and (2.5) clarify and correct Eq. (1.2).

In particular, the departure of Eqs. (2.6) and (2.7) from equalities is an $\mathcal{O}(1)$ effect, *i.e.*, not suppressed by $SU(3)_F$ breaking. Numerically, one finds $m_{\eta'} = 0.95778$ GeV and $m_\eta = 0.547862$ GeV, so that the kinematical invariants $p_{\eta(\prime)}^2 = m_{\eta(\prime)}^2$ entering Eqs. (2.6) and (2.7) differ by more than a factor of 3.

Note that this fact leads to $D \rightarrow P\eta'$ decays being uncorrelated to $D \rightarrow P\eta$ decays in $SU(3)_F$ analyses, because the corresponding matrix elements are unrelated under $SU(3)_F$. This could only be changed by putting model-dependent assumptions about the scaling of

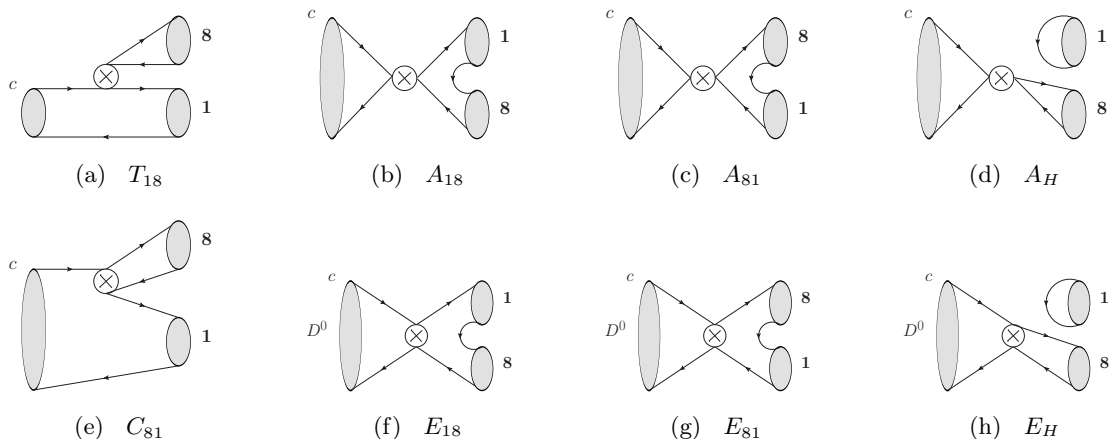


Figure 1. Topologies that contribute to $D \rightarrow P\eta'$ in the $SU(3)_F$ limit. We distinguish whether the η_1 singlet is formed from the outgoing quark or antiquark with the labels 18 and 81, respectively. The topology T_{81} does not exist due to charge conservation. The diagram C_{18} does exist but does not enter here because the weak interaction produces the quark-antiquark pair in a U -spin triplet, while the η_0 is a singlet state. The index H denotes the hairpin diagrams.

the matrix elements w.r.t. kinematical variables into place. Here, we refrain from making such assumptions and therefore focus on $D \rightarrow P\eta'$ decays only. A study of $D \rightarrow P\eta$ decays in conjunction with all $D \rightarrow PP'$ modes is left for future work.

For the mixing between the states, we assume that the mixing angle is linear in the $SU(3)_F$ breaking parameter $\varepsilon \sim 30\%$, entailing

$$\theta = \mathcal{O}(\varepsilon), \quad (2.8)$$

and implying

$$\sin \theta = \mathcal{O}(\varepsilon), \quad (2.9)$$

$$\cos \theta = 1 - \mathcal{O}(\varepsilon^2), \quad (2.10)$$

and

$$|\eta\rangle = |\eta_8\rangle + \mathcal{O}(\varepsilon), \quad (2.11)$$

$$|\eta'\rangle = |\eta_0\rangle + \mathcal{O}(\varepsilon). \quad (2.12)$$

As $\sin \theta$ always appears together with the $\mathcal{O}(1)$ hadronic matrix elements $\langle P\eta_8 | H | D \rangle'$, we will absorb the mixing angles into the matrix elements in our fit.

3 $SU(3)_F$ Decomposition of $D \rightarrow P\eta'$ decays

3.1 Topological Decomposition

Our conventions for the meson states are given in Appendix A. In the $SU(3)_F$ limit and neglecting CKM-subleading contributions, the $D \rightarrow P\eta'$ decays where $P = \pi, K, \eta$ are

parametrized by the topological tree (T), annihilation (A), colour-suppressed (C) and exchange (E) like amplitudes shown in Fig. 1. The circle with a cross denotes the W -boson exchange of the weak interaction. In addition, in the $SU(3)_F$ analysis, when breaking effects are included, it is important to differentiate whether the η_1 singlet is formed from the outgoing quark or antiquark, which we label with indices 18 and 81, respectively. We note that this distinction is rarely seen in the literature, but also only necessary when including $SU(3)_F$ breaking effects. This will become more clear through the redefinitions in Eqs. (3.4) and (3.5) below. We also note that T_{81} does not exist due to charge conservation. The topology C_{18} does exist, but does not enter due to the CKM structure of the decays. For A and E , we need also to include the corresponding hairpin diagrams, which we label by the index H .

We write the amplitudes of the Cabibbo-favoured (CF), singly Cabibbo-suppressed (SCS) and doubly Cabibbo-suppressed (DCS) $D \rightarrow P\eta'$ decays as [33]

$$\begin{aligned}\mathcal{A}^{\text{CF}}(d) &\equiv V_{cs}^*V_{ud}\mathcal{A}(d) \equiv V_{cs}^*V_{ud}\sum_i c_i^d\mathcal{T}_i, \\ \mathcal{A}^{\text{SCS}}(d) &\equiv \lambda_{sd}\mathcal{A}(d) \equiv \lambda_{sd}\sum_i c_i^d\mathcal{T}_i, \\ \mathcal{A}^{\text{DCS}}(d) &\equiv V_{cd}^*V_{us}\mathcal{A}(d) \equiv V_{cd}^*V_{us}\sum_i c_i^d\mathcal{T}_i,\end{aligned}\tag{3.1}$$

where $\lambda_{sd} = (\lambda_s - \lambda_d)/2 = (V_{cs}^*V_{us} - V_{cd}^*V_{ud})/2 \simeq \lambda_s \simeq -\lambda_d$. In this work, we neglect CKM-subleading effects, *i.e.* we set $\lambda_b = V_{cb}^*V_{ub} = 0$, as they have a negligible effect on the branching ratios. For the different decay modes $d = D \rightarrow P\eta'$, the coefficients c_i^d multiply the different topological amplitudes \mathcal{T}_i . In the $SU(3)_F$ -limit, these coefficients are listed in Table 1.

Employing the same normalization as in Ref. [33], the branching ratio is then obtained as

$$\mathcal{B}(D \rightarrow P\eta') = |\mathcal{A}^X(D \rightarrow P\eta')|^2 \times \mathcal{P}(D \rightarrow P\eta'),\tag{3.2}$$

with the phase-space function

$$\mathcal{P}(D \rightarrow P\eta') = \frac{\tau_D}{16\pi m_D^3} \times \sqrt{(m_D^2 - (m_P - m_{\eta'})^2)(m_D^2 - (m_P + m_{\eta'})^2)},\tag{3.3}$$

and where X refers to CF, SCS and DCS, indicating the CKM suppression given in Eq. (3.1).

From Table 1, we observe that in the $SU(3)_F$ -limit the eight $D \rightarrow P\eta'$ decays are split into two sections. The table has rank two, meaning that there are linear dependences in our parameterization. Absorbing these linear dependent parameters, we can redefine the “tree” and “color-suppressed” parameters:

$$\hat{T}_{18} = T_{18} + A_{18} + A_{81} + 3A_H,\tag{3.4}$$

$$\hat{C}_{81} = C_{81} + E_{18} + E_{81} + 3E_H.\tag{3.5}$$

These linear dependences are also reflected in two sets of amplitude level sum rules, namely

$$\mathcal{A}(D^+ \rightarrow K^+\eta') = \mathcal{A}(D_s^+ \rightarrow \pi^+\eta') = \mathcal{A}(D_s^+ \rightarrow K^+\eta') = -\mathcal{A}(D^+ \rightarrow \pi^+\eta'),\tag{3.6}$$

Decay ampl. $\mathcal{A}(d)$	T_{18}	A_{18}	A_{81}	A_H	C_{81}	E_{18}	E_{81}	E_H
SCS								
$\mathcal{A}(D^0 \rightarrow \pi^0 \eta')$	0	0	0	0	$\frac{1}{\sqrt{6}}$	$\frac{1}{\sqrt{6}}$	$\frac{1}{\sqrt{6}}$	$\sqrt{\frac{3}{2}}$
$\mathcal{A}(D^0 \rightarrow \eta \eta')$	0	0	0	0	$-\frac{1}{\sqrt{2}}$	$-\frac{1}{\sqrt{2}}$	$-\frac{1}{\sqrt{2}}$	$-\frac{3}{\sqrt{2}}$
$\mathcal{A}(D^+ \rightarrow \pi^+ \eta')$	$-\frac{1}{\sqrt{3}}$	$-\frac{1}{\sqrt{3}}$	$-\frac{1}{\sqrt{3}}$	$-\sqrt{3}$	0	0	0	0
$\mathcal{A}(D_s^+ \rightarrow K^+ \eta')$	$\frac{1}{\sqrt{3}}$	$\sqrt{\frac{1}{3}}$	$\frac{1}{\sqrt{3}}$	$\sqrt{3}$	0	0	0	0
CF								
$\mathcal{A}(D^0 \rightarrow \bar{K}^0 \eta')$	0	0	0	0	$\frac{1}{\sqrt{3}}$	$\frac{1}{\sqrt{3}}$	$\frac{1}{\sqrt{3}}$	$\sqrt{3}$
$\mathcal{A}(D_s^+ \rightarrow \pi^+ \eta')$	$\frac{1}{\sqrt{3}}$	$\frac{1}{\sqrt{3}}$	$\frac{1}{\sqrt{3}}$	$\sqrt{3}$	0	0	0	0
DCS								
$\mathcal{A}(D^0 \rightarrow K^0 \eta')$	0	0	0	0	$\frac{1}{\sqrt{3}}$	$\frac{1}{\sqrt{3}}$	$\frac{1}{\sqrt{3}}$	$\sqrt{3}$
$\mathcal{A}(D^+ \rightarrow K^+ \eta')$	$\frac{1}{\sqrt{3}}$	$\frac{1}{\sqrt{3}}$	$\frac{1}{\sqrt{3}}$	$\sqrt{3}$	0	0	0	0

Table 1. $SU(3)_F$ limit decomposition of $D \rightarrow P\eta'$ decays.

and

$$\mathcal{A}(D^0 \rightarrow K^0 \eta') = \mathcal{A}(D^0 \rightarrow \bar{K}^0 \eta') = \sqrt{2}\mathcal{A}(D^0 \rightarrow \pi^0 \eta') = -\sqrt{\frac{2}{3}}\mathcal{A}(D^0 \rightarrow \eta \eta'). \quad (3.7)$$

The experimental branching ratios allow for a direct test of the $SU(3)_F$ -limit sum rules when correcting for phase-space effects and CKM factors, which we show below in Sec. 4.4. In principle, the T_{18} amplitude could be estimated in the large N_c limit as done in Ref. [34]. However, T_{18} cannot be extracted unambiguously by itself from experimental data due to the redefinition in Eq. (3.4) and therefore such a comparison with theoretical estimates is not feasible.

3.2 Linear $SU(3)_F$ -breaking

We include linear $SU(3)_F$ breaking following the formalism of Refs. [33, 56]. The $SU(3)_F$ -breaking part of the Hamiltonian is given as

$$H_{\overline{SU(3)_F}} = (m_s - m_d)\bar{s}s, \quad (3.8)$$

for which the Feynman rule is denoted by a cross on the s -quark line. Furthermore, we denote the linear $SU(3)_F$ -breaking topologies with a superscript “(1)”. The diagrammatic definitions of the $SU(3)_F$ -breaking topologies are given in Appendix B. The perturbation $H_{\overline{SU(3)_F}}$ also introduces the η - η' mixing. Therefore, we treat the η_8 contribution to the η' at the same level in the power counting. Such contributions, coming from the octet contribution to the η' , are labelled with the subscript “88”.

At the first order of the expansion in $SU(3)_F$ -breaking effects also appears the broken penguin [31], *i.e.* the combination of penguin-contractions of the tree operator $P_{\text{break}} \equiv P_s - P_d$.

Decay ampl. $\mathcal{A}(d)$	\hat{T}_{18}	$\hat{T}_{18,1}^{(1)}$	$\hat{T}_{18,2}^{(1)}$	$\hat{T}_{88}^{(1)}$	$\hat{C}_{18,1}^{(1)}$	\hat{C}_{81}	$\hat{C}_{81,1}^{(1)}$	$\hat{C}_{81,2}^{(1)}$	$\hat{C}_{88}^{(1)}$
SCS									
$\mathcal{A}(D^0 \rightarrow \pi^0 \eta')$	0	0	0	0	$\frac{1}{\sqrt{6}}$	$\frac{1}{\sqrt{6}}$	0	0	$-\frac{1}{\sqrt{3}}$
$\mathcal{A}(D^0 \rightarrow \eta \eta')$	0	0	0	0	$\frac{1}{3\sqrt{2}}$	$-\frac{1}{\sqrt{2}}$	$-\frac{\sqrt{2}}{3}$	$-\frac{\sqrt{2}}{3}$	-1
$\mathcal{A}(D^+ \rightarrow \pi^+ \eta')$	$-\frac{1}{\sqrt{3}}$	0	0	$-\frac{1}{\sqrt{6}}$	$\frac{1}{\sqrt{3}}$	0	0	0	$-\sqrt{\frac{3}{2}}$
$\mathcal{A}(D_s^+ \rightarrow K^+ \eta')$	$\frac{1}{\sqrt{3}}$	$\frac{1}{\sqrt{3}}$	$\frac{1}{\sqrt{3}}$	$-\sqrt{\frac{2}{3}}$	$\frac{1}{\sqrt{3}}$	0	0	0	$-\sqrt{\frac{3}{2}}$
CF									
$\mathcal{A}(D^0 \rightarrow \bar{K}^0 \eta')$	0	0	0	0	0	$\frac{1}{\sqrt{3}}$	$\frac{1}{\sqrt{3}}$	0	$\frac{1}{\sqrt{6}}$
$\mathcal{A}(D_s^+ \rightarrow \pi^+ \eta')$	$\frac{1}{\sqrt{3}}$	$\frac{1}{\sqrt{3}}$	0	$-\sqrt{\frac{2}{3}}$	0	0	0	0	0
DCS									
$\mathcal{A}(D^0 \rightarrow \bar{K}^0 \eta')$	0	0	0	0	0	$\frac{1}{\sqrt{3}}$	0	$\frac{1}{\sqrt{3}}$	$\frac{1}{\sqrt{6}}$
$\mathcal{A}(D^+ \rightarrow K^+ \eta')$	$\frac{1}{\sqrt{3}}$	0	$\frac{1}{\sqrt{3}}$	$\frac{1}{\sqrt{6}}$	0	0	0	0	0

Table 2. $SU(3)_F$ -breaking decomposition of $D \rightarrow P\eta'$ decays including parameter redefinitions.

We give the corresponding $SU(3)_F$ -breaking decomposition of the eight $D \rightarrow P\eta'$ decays in Appendix B. As in the $SU(3)_F$ -limit case, there are linear dependent columns, meaning that our parametrization contains redundant parameters which can not be disentangled through a fit to the data. The combination of the $SU(3)_F$ limit and first order $SU(3)_F$ breaking matrix has rank six, smaller than the number of parameters.

As it is not possible to determine these parameters from theory calculations, we redefine several parameters in order to remove flat directions in the fit as much as possible. We identify the flat directions by calculating the nullspace of the $SU(3)_F$ -breaking matrix, see Refs. [26, 33] for more details.

We find the following redefinitions:

$$\hat{T}_{18,1}^{(1)} = T_{18,1}^{(1)} + T_{18,3}^{(1)} + A_{18,1}^{(1)} + A_{81,1}^{(1)} + 3A_{H,1}^{(1)} + 3\sqrt{2}A_{88}^{(1)} + 3\sqrt{2}E_{88}^{(1)}, \quad (3.9)$$

$$\hat{T}_{18,2}^{(1)} = T_{18,2}^{(1)} + A_{18,2}^{(1)} + A_{81,2}^{(1)} + A_{81,3}^{(1)} + 3A_{H,2}^{(1)} - \frac{3}{\sqrt{2}}A_{88}^{(1)} - \frac{3}{\sqrt{2}}E_{88}^{(1)}, \quad (3.10)$$

$$\hat{T}_{88}^{(1)} = T_{88}^{(1)} + 2A_{88}^{(1)} + 3E_{88}^{(1)}, \quad (3.11)$$

$$\hat{C}_{18,1}^{(1)} = C_{18,1}^{(1)} + C_{18,2}^{(1)} + P_{18,\text{break}}^{(1)} + P_{81,\text{break}}^{(1)}, \quad (3.12)$$

$$\hat{C}_{81,1}^{(1)} = C_{81,1}^{(1)} + E_{18,1}^{(1)} + E_{18,3}^{(1)} + E_{81,1}^{(1)} + 3E_{H,1}^{(1)}, \quad (3.13)$$

$$\hat{C}_{81,2}^{(1)} = C_{81,2}^{(1)} + E_{18,2}^{(1)} + E_{81,2}^{(1)} + E_{81,3}^{(1)} + 3E_{H,2}^{(1)}, \quad (3.14)$$

$$\hat{C}_{88}^{(1)} = C_{88}^{(1)} - E_{88}^{(1)}. \quad (3.15)$$

In terms of these parameters, the matrix in Appendix B can be equivalently, but much simpler, be written as the matrix in Table 2.

In principle, additional redefinitions would be possible, however these would mix $SU(3)_F$

limit parameters with $SU(3)_F$ -breaking matrix elements. In order to keep the power counting simple, we decide not to perform these additional redefinitions.

For these eight decays, we find two sum rules that also hold with $SU(3)_F$ breaking:

$$\mathcal{A}(D^+ \rightarrow K^+ \eta') + \mathcal{A}(D_s^+ \rightarrow \pi^+ \eta') - \mathcal{A}(D_s^+ \rightarrow K^+ \eta') + \mathcal{A}(D^+ \rightarrow \pi^+ \eta') = 0, \quad (3.16)$$

and

$$\mathcal{A}(D^0 \rightarrow K^0 \eta') + \mathcal{A}(D^0 \rightarrow \bar{K}^0 \eta') - \frac{\mathcal{A}(D^0 \rightarrow \pi^0 \eta')}{\sqrt{2}} + \sqrt{\frac{3}{2}} \mathcal{A}(D^0 \rightarrow \eta \eta') = 0, \quad (3.17)$$

in agreement with Ref. [30]. The number of sum rules together with the number of decay channels determines the number of linearly independent parameters. Therefore, the above sum rules also imply agreement with the matrix rank of the corresponding coefficient tables found in the group-theoretical approach in Ref. [30].

4 Numerical Results

4.1 Constraining diagrammatic $SU(3)_F$ breaking

We impose constraints on the $SU(3)_F$ -breaking part of the amplitude through

$$\left| \frac{\mathcal{A}_{\cancel{SU(3)}}(D \rightarrow P\eta')}{\mathcal{A}_{SU(3)\text{-lim}}(D \rightarrow P\eta')} \right| \leq \varepsilon, \quad (4.1)$$

where $\mathcal{A}_{\cancel{SU(3)}}$ corresponds to the part of the amplitude arising only from the $SU(3)_F$ -breaking terms in the amplitude, $\mathcal{A}_{SU(3)\text{-lim}}$ refers to the $SU(3)_F$ limit part of the amplitude, and ε is the imposed amount of allowed $SU(3)_F$ breaking. This constraint is applied to all eight $D \rightarrow P\eta'$ channels. We note that our treatment of $SU(3)_F$ breaking differs from Refs. [26, 34], where also the $SU(3)_F$ -breaking of individual parameters has been constrained. Due to the redefinitions in Eq. (3.15), the different topologies mix to a large amount, making such a constraint less intuitive. Therefore, we only constrain the effect of $SU(3)_F$ breaking on an amplitude as a whole, and not its individual contributions. Commonly it is expected that $\varepsilon \sim 20\%$ – 30% , motivated from the ratio of decay constants $f_K/f_\pi - 1 \sim 20\%$ [57].

We emphasize that our constraint on $SU(3)_F$ -breaking in Eq. (4.1) requires the separation of $SU(3)_F$ -breaking and $SU(3)_F$ -limit parameters. This is possible as we do not mix these two contributions in our redefinitions Eqs. (3.4), (3.5), and (3.9)–(3.15). Importantly, the form of the employed constraint on $SU(3)_F$ breaking and of the redefinitions ensure that our redefinitions are merely a technical way to simplify the fit and do not affect the fit results for observables, *i.e.* branching ratios.

4.2 Fit setup and $SU(3)_F$ test

In our global fit, we use the measured branching ratios given in Table 3. Masses and lifetimes are taken from Ref. [58] and for the CKM factors we use the Wolfenstein parametrization up to λ^2 with $\lambda = 0.225$ [58]. The theoretical parametrization for the amplitudes is given

Observable	Global theory fit	Experiment
$\mathcal{B}(D^0 \rightarrow \pi^0 \eta')$	$(9.15_{-0.99}^{+1.00}) \cdot 10^{-4}$	$(9.2 \pm 1.0) \cdot 10^{-4}$
$\mathcal{B}(D^0 \rightarrow \eta \eta')$	$(0.98 \pm 0.18) \cdot 10^{-3}$	$(1.01 \pm 0.19) \cdot 10^{-3}$
$\mathcal{B}(D^+ \rightarrow \pi^+ \eta')$	$(4.95 \pm 0.19) \cdot 10^{-3}$	$(4.97 \pm 0.19) \cdot 10^{-3}$
$\mathcal{B}(D_s^+ \rightarrow K^+ \eta')$	$(2.22 \pm 0.17) \cdot 10^{-3}$	$(2.64 \pm 0.24) \cdot 10^{-3}$
$\mathcal{B}(D^0 \rightarrow K_S \eta')$	$(9.56_{-0.25}^{+0.27}) \cdot 10^{-3}$	$(9.49 \pm 0.32) \cdot 10^{-3}$
$\mathcal{B}(D^0 \rightarrow K_L \eta')$	$(8.04_{-0.29}^{+0.26}) \cdot 10^{-3}$	$(8.12 \pm 0.35) \cdot 10^{-3}$
$\mathcal{B}(D_s^+ \rightarrow \pi^+ \eta')$	$(4.17 \pm 0.23) \cdot 10^{-2}$	$(3.94 \pm 0.25) \cdot 10^{-2}$
$\mathcal{B}(D^+ \rightarrow K^+ \eta')$	$(2.11 \pm 0.17) \cdot 10^{-4}$	$(1.85 \pm 0.20) \cdot 10^{-4}$

Table 3. Comparison of experimental input data from Ref. [58] to our global theory fit allowing for 30% $SU(3)_F$ breaking. All shown errors are 1σ uncertainties. The experimental data are uncorrelated with the exception of $\mathcal{B}(D^+ \rightarrow K^+ \eta')$ and $\mathcal{B}(D^+ \rightarrow \pi^+ \eta')$, which have a correlation coefficient of 0.32 [58].

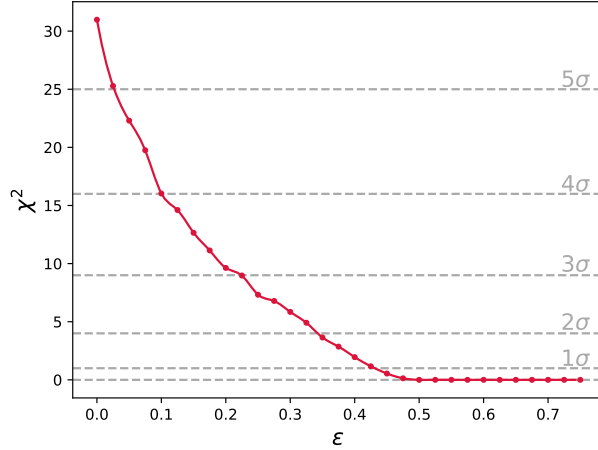


Figure 2. Minimum χ^2 value as a function of the imposed $SU(3)_F$ breaking constraint ε at the amplitude level. Starting at $\varepsilon = 50\%$, there is a perfect description of the data.

in Table 2, giving in total 17 fit parameters for eight observables. In the $SU(3)_F$ -limit, we have only three parameters

$$|\hat{T}_{18}|, \quad |\hat{C}_{81}/\hat{T}_{18}|, \quad \arg(\hat{C}_{81}), \quad (4.2)$$

where the absolute phase of \hat{T}_{18} is undetermined and without loss of generality set to zero. For convenience, we normalize all parameters to \hat{T}_{18} . For the $SU(3)_F$ -breaking parameters, we then have

$$|\hat{T}_{18,1}^{(1)}/\hat{T}_{18}|, \quad \arg(\hat{T}_{18,1}^{(1)}), \quad |\hat{T}_{18,2}^{(1)}/\hat{T}_{18}|, \quad \arg(\hat{T}_{18,2}^{(1)}), \quad |\hat{T}_{88}^{(1)}/\hat{T}_{18}|, \quad \arg(\hat{T}_{88}^{(1)}), \quad (4.3)$$

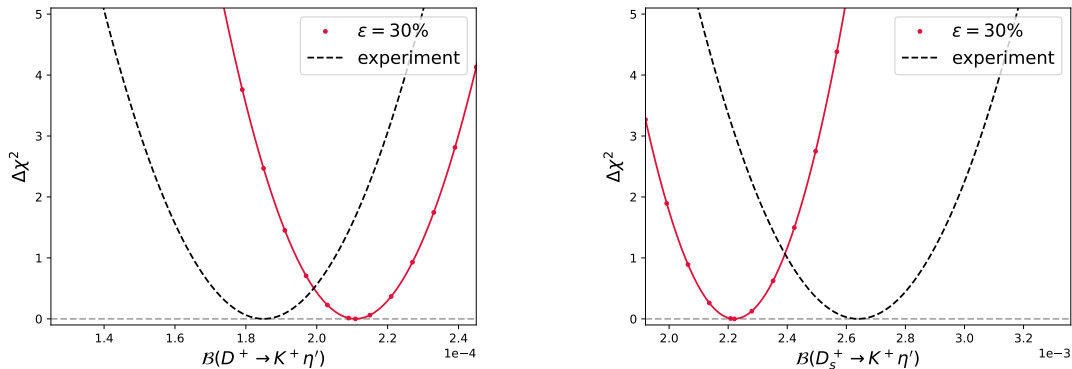


Figure 3. Branching ratio scans for the global theory fit with $\varepsilon = 30\%$ (red) compared to the experimental results (black) for $D^+ \rightarrow K^+\eta'$ (left) and $D_s^+ \rightarrow K^+\eta'$ (right).

and

$$\begin{aligned}
 & |\hat{C}_{81,1}^{(1)}/\hat{T}_{18}|, \quad \arg(\hat{C}_{81,1}^{(1)}), \quad |\hat{C}_{81,2}^{(1)}/\hat{T}_{18}|, \quad \arg(\hat{C}_{81,2}^{(1)}), \\
 & |\hat{C}_{18,1}^{(1)}/\hat{T}_{18}|, \quad \arg(\hat{C}_{18,1}^{(1)}), \quad |\hat{C}_{88}^{(1)}/\hat{T}_{18}|, \quad \arg(\hat{C}_{88}^{(1)}).
 \end{aligned} \tag{4.4}$$

We then perform a χ^2 minimisation by constructing

$$\chi^2 = (\vec{y}_{\text{data}} - \vec{y}_{\text{theo}})^T \text{Cov}^{-1} (\vec{y}_{\text{data}} - \vec{y}_{\text{theo}}). \tag{4.5}$$

Every minimisation is performed 100 times starting from randomised initial starting points for the parameters in order to avoid local minima of the function. We include the $SU(3)_F$ -breaking constraints of Eq. (4.1) in a frequentist analysis using the Sequential Least Squares Programming (SLSQP) algorithm implemented in SciPy [59, 60].

To test our $SU(3)_F$ assumption, we first perform a scan of the value of χ^2 with respect to the imposed $SU(3)_F$ -breaking constraint, ε . This scan is shown in Fig. 2, where we also indicate $\chi^2 = 1, 4, 9, 16, 25$ lines. We note that the identification of those lines with CLs is ambiguous, as the number of degrees of freedom is not well-defined. In the following we count the constraint on $SU(3)_F$ breaking as one degree of freedom. This procedure could be improved using toy Monte Carlo data with a Feldman-Cousins approach, which is beyond the scope of our paper. We obtain a perfect fit to the experimental data for $\varepsilon \geq 50\%$ where we obtain $\chi^2 = 0$. At the same time, we note that such a large amount of $SU(3)_F$ breaking in principle violates our initial assumption to consider only linear $SU(3)_F$ breaking. The $SU(3)_F$ -limit fit, where $\varepsilon = 0$, has $\chi^2 = 31.4$, about half of this comes from the $D^0 \rightarrow \pi^0\eta'$ decay, which we comment on later. Comparing to the scenario that gives $\chi^2 = 0$ ($\varepsilon \geq 50\%$) excludes the $SU(3)_F$ limit therefore at 5.6σ . It is therefore clear that $SU(3)_F$ -breaking has to be taken into account.

Our nominal result corresponds to $\varepsilon = 30\%$, with $\chi^2 = 6.01$, in slight tension of 2.5σ with the data when compared to the fit with $\varepsilon = 50\%$ (i.e. $\chi^2 = 0$).

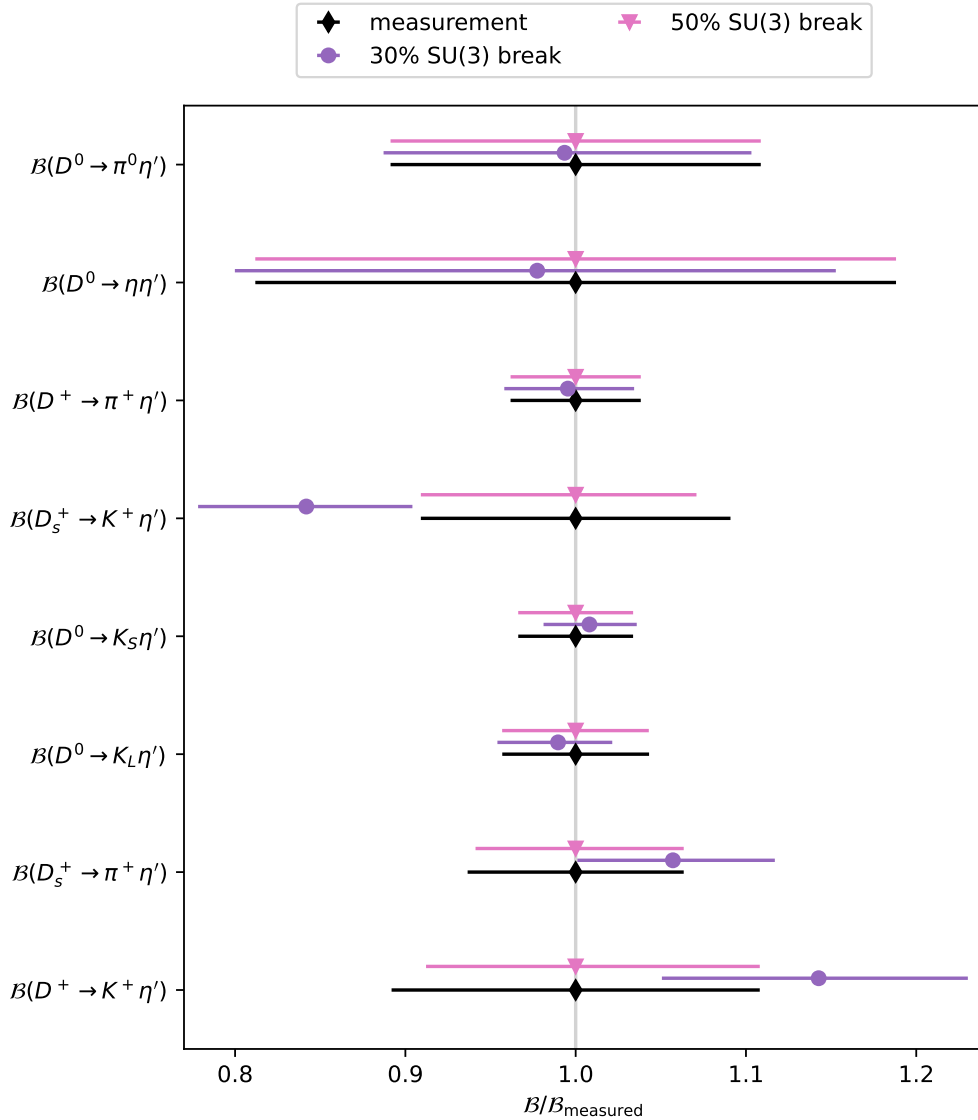


Figure 4. Comparison of experimental input data (black) with the results of our global fit allowing for 30% $SU(3)_F$ breaking (purple) and 50% $SU(3)_F$ breaking (pink). All branching ratios are normalised to the central value of the experimental results.

4.3 Implications for branching ratios

As already discussed, due to the multiple redefinitions of the underlying theory parameters, their interpretability is limited. We therefore concentrate here on the implications of our global fit for the branching ratios. To do so, we compute $\Delta\chi^2$ profiles of the branching ratios, comparing to the global minimum with a fixed value for ε . The 1σ uncertainties are determined from the criterion $\Delta\chi^2 = 1$. Examples of these scans for our nominal $\varepsilon = 30\%$ fit can be seen in Fig. 3 for the decays $D_{(s)}^+ \rightarrow K^+ \eta'$. A summary of all theoretical fit results

are quoted in Table 3. In Fig. 4, we compare our nominal fit results with the experimental data. All branching ratios are normalized to the central value of the experimental result. In addition, we also show the results from a fit with 50% $SU(3)_F$ breaking. In the latter case, we find excellent agreement with the experimental data and similar uncertainties, *i.e.* in this case we basically only reproduce the data. For our nominal fit, for $D_s^+ \rightarrow K^+\eta'$ we find a 1.4σ deviation from the experimental result. Also $D^+ \rightarrow K^+\eta'$ and $D_s^+ \rightarrow \pi^+\eta'$ show a difference of 1.0 and 0.7σ , respectively. Improved branching ratio measurements of these decays would thus be useful to obtain more information on the amount of $SU(3)_F$ breaking. In addition, $D \rightarrow \pi^0\eta'$ and $D^0 \rightarrow \eta\eta'$ are only known at the 10% level, making updates of these modes also highly desirable.

4.4 Theory correlations between branching ratios

Besides the global fit results for the individual branching ratios, it is interesting to consider correlations between different branching ratios stemming from the underlying $SU(3)_F$ symmetry. In Fig. 5 and 6, we show the theory correlations between branching ratios of several neutral and charged decays, respectively. We consider the correlations between sets of charged and neutral decays because we have separate sum rules for these sets given in (3.16) and (3.17). In addition, the neutral and charged modes are completely separate systems in the $SU(3)_F$ limit. To highlight this, we also show the $SU(3)_F$ -limit relations between the respective decays. For completeness, we also show the experimental data given in Table 3.

In Fig. 5, we give the correlation between the SCS modes ($D^0 \rightarrow \pi^0\eta'$, $D^0 \rightarrow \eta\eta'$). Interestingly, we observe that these decays, while being in perfect agreement with the experimental data, differ significantly from the $SU(3)_F$ -limit prediction. For the modes with a neutral K^0 , observed through their physical K_S and K_L states, we consider the correlation between ($D^0 \rightarrow K_S\eta'$, $D^0 \rightarrow K_L\eta'$). In the $SU(3)_F$ -limit, the branching ratios of these decays are given by

$$\begin{aligned}\mathcal{B}(D^0 \rightarrow K_S\eta') &\sim |\hat{C}_{81}|^2(1 + 2\lambda^2) + \mathcal{O}(\lambda^4), \\ \mathcal{B}(D^0 \rightarrow K_L\eta') &\sim |\hat{C}_{81}|^2(1 - 2\lambda^2) + \mathcal{O}(\lambda^4),\end{aligned}\tag{4.6}$$

because the physical states contain both CF and DCS parts. We observe that the data and our fit results in these modes are in agreement with $SU(3)_F$ -flavour symmetry. As expected, we also observe a strong theory correlation between these decays. It would therefore be interesting to also consider possible experimental correlations between these decays in future measurements.

For the charged decays, we consider several modes shown in Fig. 6. First, we show the set of SCS decays; ($D^+ \rightarrow \pi^+\eta'$, $D_s^+ \rightarrow K^+\eta'$) and combine the CF and DCS modes; ($D_s^+ \rightarrow \pi^+\eta'$, $D^+ \rightarrow K^+\eta'$). Although these decays are described largely by the same parameters (see Table 2), we do not observe strong correlations in our theory predictions.

For completeness, we also show the correlations between decays with the same initial D^+ and D_s^+ state: ($D^+ \rightarrow \pi^+\eta'$, $D^+ \rightarrow K^+\eta'$) and ($D_s^+ \rightarrow \pi^+\eta'$, $D_s^+ \rightarrow K^+\eta'$). For the latter, we notice also a clear deviation of the experimental measurements and the $SU(3)_F$ -

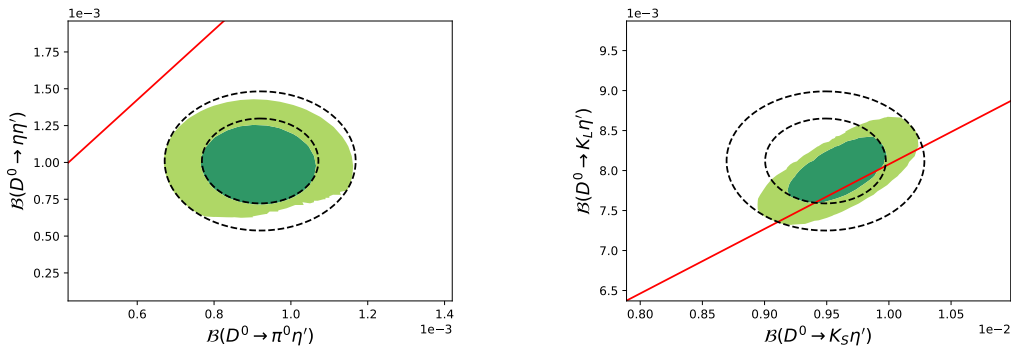


Figure 5. Correlations between branching ratios of the neutral modes. The red line represents the $SU(3)_F$ limit sum rule. The shaded areas correspond to the global fit result and the black lines to the experimental determinations. Contour lines represent the 68.30% and 95.45% confidence levels.

limit correlation. Last, we show the correlation between $(D_s^+ \rightarrow K^+\eta', D^+ \rightarrow K^+\eta')$, because these decays show the largest tension with the experimental results.

The two-dimensional correlations in Fig. 5 and Fig. 6 clearly show how several sets of decays deviate (or agree with) the $SU(3)_F$ -limit sum rules. Therefore, it would be interesting to have more precise corresponding branching ratio measurements in the future including their correlations.

5 Conclusions

We presented a first study of $SU(3)_F$ -breaking effects in $D \rightarrow P\eta'$ using a consistent treatment of the singlet-octet mixing between η_0 and η_8 within the $SU(3)_F$ power counting. Our universal mixing angle θ is not an observable quantity, unavoidably θ always appears together with the matrix elements. As a consequence $D \rightarrow P\eta'$ decays become uncorrelated to $D \rightarrow P\eta$. We find that the $SU(3)_F$ limit is ruled out by the data at 5.6σ when compared to a fit with 50% $SU(3)_F$ breaking, which gives a perfect description of the data. Allowing for 30% $SU(3)_F$ breaking at the amplitude level, we show that the data can be consistently described. From the underlying theoretical expansion, we are able to predict the eight $D \rightarrow P\eta'$ branching ratios and the correlations between several decay channels.

We find 1σ differences between our theoretical prediction and measurements of the channels $D_s \rightarrow K^+\eta'$ and $D^+ \rightarrow K^+\eta'$. We predict that if $SU(3)_F$ -breaking is 30% or smaller, we predict that future measurements of the branching ratio of $D_s \rightarrow K^+\eta'$ go down and $D^+ \rightarrow K^+\eta'$ go up. If on the contrary, future measurements do not show this trend, we have to conclude that $SU(3)_F$ breaking is larger than expected. As such, updated measurements of these decays are highly desired to shed further light on $SU(3)_F$ -breaking effects in the charm sector. We point out that especially the two-dimensional correlations between sets of charged or neutral decays can clearly show whether $SU(3)_F$ symmetry is respected (or broken) in subsets of decays. Doing so, we found that the channels $D^0 \rightarrow \pi^0\eta'$ and $D^0 \rightarrow \eta\eta'$ show the largest deviation from the $SU(3)_F$ limit. Clearly such decays are

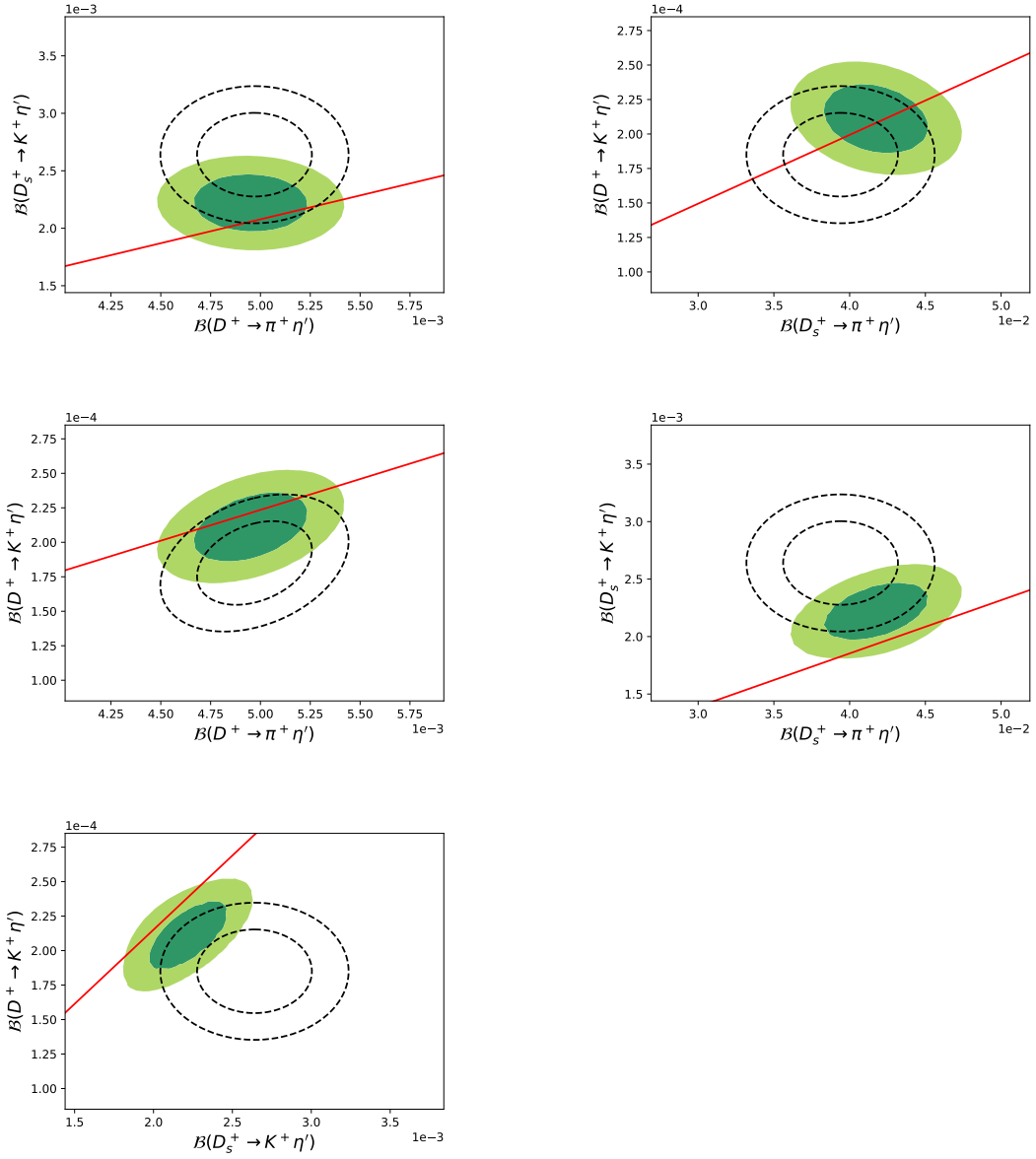


Figure 6. Correlations between branching ratios for the charged modes. The red line represents the $SU(3)_F$ limit sum rule. The shaded areas correspond to the global fit result and the black lines to the experimental determinations. Contour lines represent the 68.30% and 95.45% confidence levels.

challenging to measure, but we emphasize that improved measurements of their branching ratios would allow to further test the quality of $SU(3)_F$ symmetry in the charm sector.

Our thorough analysis of $D \rightarrow P\eta'$ serves as a first step towards predicting CP asymmetries in these modes. Finally, it would be interesting to compare our analysis with an updated analysis of $SU(3)_F$ breaking in the $D \rightarrow PP$ modes (including the η channels) which is currently in progress [61].

Acknowledgments

S.S. is supported by a Stephen Hawking Fellowship from UKRI under reference EP/T01623X/1 and the STFC research grant ST/X00077X/1. The work of K.K.V. is supported in part by the Dutch Research Council (NWO) as part of the project Solving Beautiful Puzzles (VI.Vidi.223.083) of the research programme Vidi. U.N. acknowledges support by BMBF grant 05H21VKKBA, *Theoretische Studien für Belle II und LHCb*.

A Notation

We employ the following sign convention

$$|K^+\rangle = |u\bar{s}\rangle, \quad |K^0\rangle = |d\bar{s}\rangle, \quad (\text{A.1})$$

$$|K^-\rangle = |s\bar{u}\rangle, \quad |\bar{K}^0\rangle = |s\bar{d}\rangle, \quad (\text{A.2})$$

$$|\pi^+\rangle = |u\bar{d}\rangle, \quad |\pi^0\rangle = \frac{1}{\sqrt{2}}(|u\bar{u}\rangle - |d\bar{d}\rangle), \quad (\text{A.3})$$

$$|\pi^-\rangle = |d\bar{u}\rangle, \quad |D^0\rangle = |c\bar{u}\rangle, \quad (\text{A.4})$$

$$|D^+\rangle = |c\bar{d}\rangle, \quad |D_s^+\rangle = |c\bar{s}\rangle, \quad (\text{A.5})$$

found from $M^a \sim (\bar{u}, \bar{d}, \bar{s})\lambda^a(u, d, s)^T$ with the Gell-Mann matrices λ^a and $|\pi^-\rangle = |M^-\rangle = |M^1 + iM^2\rangle/2$, $|\pi^0\rangle = |M^3\rangle/\sqrt{2}$, and so on. Note that this sign convention deviates from the one used in other works [33, 34, 62]. The meson octet thus corresponds to

$$|\pi^+\rangle, |\pi^0\rangle, |\pi^-\rangle, |K^+\rangle, |K^0\rangle, |\bar{K}^0\rangle, |K^-\rangle, |\eta_8\rangle. \quad (\text{A.6})$$

For the K_S and K_L decays, we write the physical states as

$$|K_S\rangle = \frac{|K^0\rangle - |\bar{K}^0\rangle}{\sqrt{2}}, \quad |K_L\rangle = \frac{|K^0\rangle + |\bar{K}^0\rangle}{\sqrt{2}}, \quad (\text{A.7})$$

which mixes the CF and DCS amplitudes.

Here $C|K^0\rangle = |\bar{K}^0\rangle$, *i.e.* $CP|K^0\rangle = -|\bar{K}^0\rangle$ is used. The sign convention for the charge conjugation operation C is linked to the conventions in Eq. (A.5), because one can transform $|K^0\rangle$ into $|\bar{K}^0\rangle$ in two ways, by applying C or by rotating the state around the y -axis in U-spin space with angle π , and both transformations must be compatible with each other [33]. If one erroneously exchanges the "-" and "+" signs in Eq. (A.7), one will find the wrong hierarchy among the branching fractions in Eq. (4.6). The combination of the mentioned U-spin rotation and C is called G_U parity [63–65], which is the analogue of Lee's and Yang's G parity based on isospin [66]. $|K^0\rangle$ and $|\bar{K}^0\rangle$ are eigenstates of G_U with eigenvalue -1 ; the requirement that all members of the U-spin triplet have the same G_U quantum number fixes the sign convention for C and implies the "-" sign in $|K_S\rangle$ in Eq. (A.7).

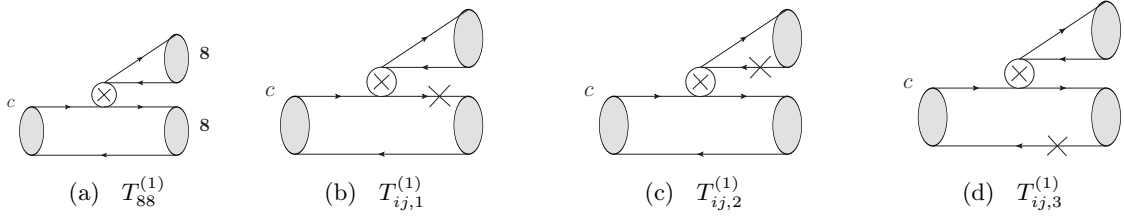


Figure 7. $SU(3)_F$ -breaking tree topologies.

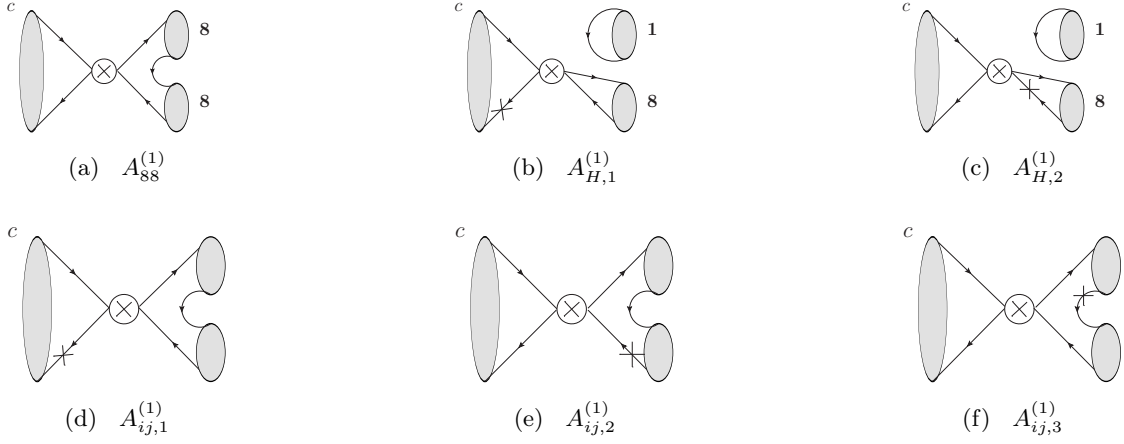


Figure 8. $SU(3)_F$ -breaking annihilation topologies.

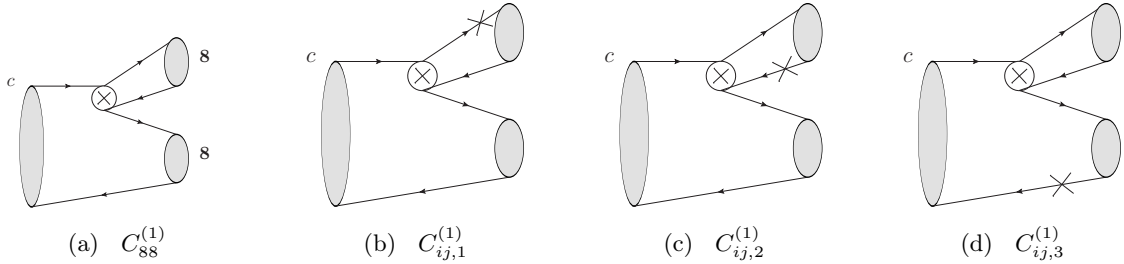


Figure 9. $SU(3)_F$ -breaking color-suppressed topologies.

B $SU(3)_F$ -breaking topological diagrams and decomposition without redefinitions

In Figs. 7–10 we show all topological Feynman diagrams with linear $SU(3)_F$ -breaking denoted with a superscript (1). We show the $SU(3)_F$ decomposition without redefinitions in Table 4.

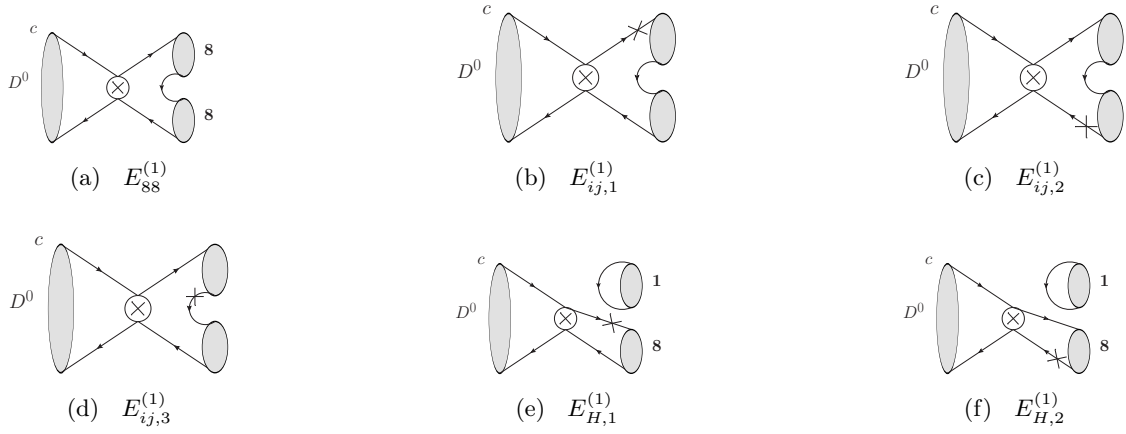


Figure 10. $SU(3)_F$ -breaking exchange topologies. The $SU(3)_F$ -breaking effects within the hairpin itself can be absorbed into the $SU(3)_F$ limit hairpin diagram. Note further that there are 3 $SU(3)_F$ breaking topologies for each of the $SU(3)_F$ limit exchange topologies, *i.e.*, a total of nine different $SU(3)_F$ breaking exchange diagrams plus two $SU(3)_F$ breaking hairpin diagrams.

Decay	$T_{18,1}^{(1)}$	$T_{18,2}^{(1)}$	$T_{18,3}^{(1)}$	$T_{88}^{(1)}$	$A_{18,1}^{(1)}$	$A_{18,2}^{(1)}$	$A_{81,1}^{(1)}$	$A_{81,2}^{(1)}$	$A_{81,3}^{(1)}$	$A_{88}^{(1)}$	$A_{H,1}^{(1)}$	$A_{H,2}^{(1)}$	$C_{18,1}^{(1)}$	$C_{18,2}^{(1)}$	$C_{81,1}^{(1)}$	$C_{81,2}^{(1)}$	$C_{88}^{(1)}$	$E_{18,1}^{(1)}$	$E_{18,2}^{(1)}$	$E_{18,3}^{(1)}$	$E_{81,1}^{(1)}$	$E_{81,2}^{(1)}$	$E_{81,3}^{(1)}$	$E_{88}^{(1)}$	$E_{H,1}^{(1)}$	$E_{H,2}^{(1)}$	$P_{18,\text{break}}^{(1)}$	$P_{81,\text{break}}^{(1)}$	
SCS																													
$D^0 \rightarrow \pi^0 \eta'$	0	0	0	0	0	0	0	0	0	0	0	0	$\frac{1}{\sqrt{6}}$	$\frac{1}{\sqrt{6}}$	0	0	$-\frac{1}{\sqrt{3}}$	0	0	0	0	0	0	$\frac{1}{\sqrt{3}}$	0	0	$\frac{1}{\sqrt{6}}$	$\frac{1}{\sqrt{6}}$	
$D^0 \rightarrow \eta \eta'$	0	0	0	0	0	0	0	0	0	0	0	0	$\frac{1}{3\sqrt{2}}$	$\frac{1}{3\sqrt{2}}$	$-\frac{\sqrt{2}}{3}$	$-\frac{\sqrt{2}}{3}$	-1	$-\frac{\sqrt{2}}{3}$	$-\frac{\sqrt{2}}{3}$	$-\frac{\sqrt{2}}{3}$	$-\frac{\sqrt{2}}{3}$	$-\frac{\sqrt{2}}{3}$	$-\frac{\sqrt{2}}{3}$	1	$-\sqrt{2}$	$-\sqrt{2}$	$\frac{1}{3\sqrt{2}}$	$\frac{1}{3\sqrt{2}}$	
$D^+ \rightarrow \pi^+ \eta'$	0	0	0	$-\frac{1}{\sqrt{6}}$	0	0	0	0	0	$-\sqrt{\frac{2}{3}}$	0	0	$\frac{1}{\sqrt{3}}$	$\frac{1}{\sqrt{3}}$	0	0	$-\sqrt{\frac{3}{2}}$	0	0	0	0	0	0	0	0	0	$\frac{1}{\sqrt{3}}$	$\frac{1}{\sqrt{3}}$	
$D_s^+ \rightarrow K^+ \eta'$	$\frac{1}{\sqrt{3}}$	$\frac{1}{\sqrt{3}}$	$\frac{1}{\sqrt{3}}$	$-\sqrt{\frac{2}{3}}$	$\frac{1}{\sqrt{3}}$	$\frac{1}{\sqrt{3}}$	$\frac{1}{\sqrt{3}}$	$\frac{1}{\sqrt{3}}$	$\frac{1}{\sqrt{3}}$	$-\frac{1}{\sqrt{6}}$	$\sqrt{3}$	$\sqrt{3}$	$\frac{1}{\sqrt{3}}$	$\frac{1}{\sqrt{3}}$	0	0	$-\sqrt{\frac{3}{2}}$	0	0	0	0	0	0	0	0	0	$\frac{1}{\sqrt{3}}$	$\frac{1}{\sqrt{3}}$	
CF																													
$D^0 \rightarrow \bar{K}^0 \eta'$	0	0	0	0	0	0	0	0	0	0	0	0	0	$\sqrt{\frac{1}{3}}$	0	$\frac{1}{\sqrt{6}}$	$\sqrt{\frac{1}{3}}$	0	$\sqrt{\frac{1}{3}}$	$\sqrt{\frac{1}{3}}$	0	0	$-\frac{1}{\sqrt{6}}$	$\sqrt{3}$	0	0	0	0	
$D_s^+ \rightarrow \pi^+ \eta'$	$\frac{1}{\sqrt{3}}$	0	$\frac{1}{\sqrt{3}}$	$-\sqrt{\frac{2}{3}}$	$\frac{1}{\sqrt{3}}$	0	$\frac{1}{\sqrt{3}}$	0	0	$\sqrt{\frac{2}{3}}$	$\sqrt{3}$	0	0	0	0	0	0	0	0	0	0	0	0	0	0	0	0	0	0
DCS																													
$D^0 \rightarrow K^0 \eta'$	0	0	0	0	0	0	0	0	0	0	0	0	0	0	$\frac{1}{\sqrt{3}}$	$\frac{1}{\sqrt{6}}$	0	$\frac{1}{\sqrt{3}}$	0	0	$\frac{1}{\sqrt{3}}$	$\frac{1}{\sqrt{3}}$	$-\frac{1}{\sqrt{6}}$	0	$\sqrt{3}$	0	0	0	
$D^+ \rightarrow K^+ \eta'$	0	$\frac{1}{\sqrt{3}}$	0	$\frac{1}{\sqrt{6}}$	0	$\frac{1}{\sqrt{3}}$	0	$\frac{1}{\sqrt{3}}$	$\frac{1}{\sqrt{3}}$	$-\frac{1}{\sqrt{6}}$	0	$\sqrt{3}$	0	0	0	0	0	0	0	0	0	0	0	0	0	0	0	0	0

Table 4. $SU(3)_F$ breaking diagrams. Note that the $SU(3)_F$ limit diagram 88 is power suppressed for η' . Note also that the diagrams $A_{18,3}^{(1)}$, $C_{18,3}^{(1)}$, $C_{81,3}^{(1)}$ do not contribute.

References

- [1] LHCb collaboration, *Observation of CP Violation in Charm Decays*, *Phys. Rev. Lett.* **122** (2019) 211803 [1903.08726].
- [2] LHCb collaboration, *Measurement of the Time-Integrated CP Asymmetry in $D^0 \rightarrow K^- K^+$ Decays*, *Phys. Rev. Lett.* **131** (2023) 091802 [2209.03179].
- [3] LHCb collaboration, *Search for CP violation in $D_{(s)}^+ \rightarrow K^- K^+ K^+$ decays*, *JHEP* **07** (2023) 067 [2303.04062].
- [4] LHCb collaboration, *Search for CP violation in the phase space of $D^0 \rightarrow \pi^- \pi^+ \pi^0$ decays with the energy test*, *JHEP* **09** (2023) 129 [2306.12746].
- [5] LHCb collaboration, *Search for CP violation in the phase space of $D^0 \rightarrow K_S^0 K^\pm \pi^\mp$ decays with the energy test*, *JHEP* **03** (2024) 107 [2310.19397].
- [6] LHCb collaboration, *Measurement of CP violation observables in $D^+ \rightarrow K^- K^+ \pi^+$ decays*, [2409.01414](#).
- [7] CMS collaboration, *Search for CP violation in $D^0 \rightarrow K_S^0 K_S^0$ decays in proton-proton collisions at $\sqrt{s} = 13$ TeV*, [2405.11606](#).
- [8] BELLE-II collaboration, *Novel method for the identification of the production flavor of neutral charmed mesons*, *Phys. Rev. D* **107** (2023) 112010 [2304.02042].
- [9] BELLE collaboration, *Search for CP violation in $D(s) \rightarrow K + KS^0 h + h^-$ ($h=K, \pi$) decays and observation of the Cabibbo-suppressed decay $Ds^+ \rightarrow K + K - KS^0 \pi^+$* , *Phys. Rev. D* **108** (2023) L111102 [2305.11405].
- [10] BELLE-II collaboration, *The Belle II Physics Book*, *PTEP* **2019** (2019) 123C01 [1808.10567].
- [11] A. Cerri et al., *Report from Working Group 4: Opportunities in Flavour Physics at the HL-LHC and HE-LHC*, *CERN Yellow Rep. Monogr.* **7** (2019) 867 [1812.07638].
- [12] LHCb collaboration, *Physics case for an LHCb Upgrade II - Opportunities in flavour physics, and beyond, in the HL-LHC era*, [1808.08865](#).
- [13] BESIII collaboration, *Measurements of absolute branching fractions of $D^0 \rightarrow K_L^0 \phi, K_L^0 \eta, K_L^0 \omega$, and $K_L^0 \eta'$* , *Phys. Rev. D* **105** (2022) 092010 [2202.13601].
- [14] BELLE collaboration, *Measurement of branching fractions and search for CP violation in $D^0 \rightarrow \pi^+ \pi^- \eta, D^0 \rightarrow K^+ K^- \eta$, and $D^0 \rightarrow \phi \eta$ at Belle*, *JHEP* **09** (2021) 075 [2106.04286].
- [15] LHCb collaboration, *Measurement of CP asymmetries in $D_{(s)}^+ \rightarrow \eta \pi^+$ and $D_{(s)}^+ \rightarrow \eta' \pi^+$ decays*, *JHEP* **04** (2023) 081 [2204.12228].
- [16] LHCb collaboration, *Search for CP violation in $D_{(s)}^+ \rightarrow h^+ \pi^0$ and $D_{(s)}^+ \rightarrow h^+ \eta$ decays*, *JHEP* **06** (2021) 019 [2103.11058].
- [17] BELLE collaboration, *Measurement of branching fractions and CP asymmetries for $D_s^+ \rightarrow K^+(\eta, \pi^0)$ and $D_s^+ \rightarrow \pi^+(\eta, \pi^0)$ decays at Belle*, *Phys. Rev. D* **103** (2021) 112005 [2103.09969].
- [18] R.L. Kingsley, S.B. Treiman, F. Wilczek and A. Zee, *Weak Decays of Charmed Hadrons*, *Phys. Rev. D* **11** (1975) 1919.
- [19] M.B. Voloshin, V.I. Zakharov and L.B. Okun, *Two particle nonleptonic decays of D and F mesons, and structure of weak interactions*, *JETP Lett.* **21** (1975) 183.

- [20] V.D. Barger and S. Pakvasa, *Two-body Hadronic Decays of D Mesons*, *Phys. Rev. Lett.* **43** (1979) 812.
- [21] M. Golden and B. Grinstein, *Enhanced CP Violations in Hadronic Charm Decays*, *Phys. Lett. B* **222** (1989) 501.
- [22] M.J. Savage and R.P. Springer, *SU(3) Predictions for Charmed Baryon Decays*, *Phys. Rev. D* **42** (1990) 1527.
- [23] F. Buccella, M. Lusignoli, G. Miele, A. Pugliese and P. Santorelli, *Nonleptonic weak decays of charmed mesons*, *Phys. Rev. D* **51** (1995) 3478 [[hep-ph/9411286](#)].
- [24] D. Pirtskhalava and P. Uttayarat, *CP Violation and Flavor SU(3) Breaking in D-meson Decays*, *Phys. Lett. B* **712** (2012) 81 [[1112.5451](#)].
- [25] B. Bhattacharya, M. Gronau and J.L. Rosner, *CP asymmetries in singly-Cabibbo-suppressed D decays to two pseudoscalar mesons*, *Phys. Rev. D* **85** (2012) 054014 [[1201.2351](#)].
- [26] G. Hiller, M. Jung and S. Schacht, *SU(3)-flavor anatomy of nonleptonic charm decays*, *Phys. Rev. D* **87** (2013) 014024 [[1211.3734](#)].
- [27] Y. Grossman, A.L. Kagan and J. Zupan, *Testing for new physics in singly Cabibbo suppressed D decays*, *Phys. Rev. D* **85** (2012) 114036 [[1204.3557](#)].
- [28] H.-Y. Cheng and C.-W. Chiang, *Direct CP violation in two-body hadronic charmed meson decays*, *Phys. Rev. D* **85** (2012) 034036 [[1201.0785](#)].
- [29] T. Feldmann, S. Nandi and A. Soni, *Repercussions of Flavour Symmetry Breaking on CP Violation in D-Meson Decays*, *JHEP* **06** (2012) 007 [[1202.3795](#)].
- [30] Y. Grossman and D.J. Robinson, *SU(3) Sum Rules for Charm Decay*, *JHEP* **04** (2013) 067 [[1211.3361](#)].
- [31] J. Brod, Y. Grossman, A.L. Kagan and J. Zupan, *A Consistent Picture for Large Penguins in $D \rightarrow \pi^+ \pi^-$, $K^+ K^-$* , *JHEP* **10** (2012) 161 [[1203.6659](#)].
- [32] U. Nierste and S. Schacht, *CP Violation in $D^0 \rightarrow K_S K_S$* , *Phys. Rev. D* **92** (2015) 054036 [[1508.00074](#)].
- [33] S. Müller, U. Nierste and S. Schacht, *Topological amplitudes in D decays to two pseudoscalars: A global analysis with linear $SU(3)_F$ breaking*, *Phys. Rev.* **D92** (2015) 014004 [[1503.06759](#)].
- [34] S. Müller, U. Nierste and S. Schacht, *Sum Rules of Charm CP Asymmetries beyond the $SU(3)_F$ Limit*, *Phys. Rev. Lett.* **115** (2015) 251802 [[1506.04121](#)].
- [35] U. Nierste and S. Schacht, *Neutral $D \rightarrow KK^*$ decays as discovery channels for charm CP violation*, *Phys. Rev. Lett.* **119** (2017) 251801 [[1708.03572](#)].
- [36] X.-G. He and W. Wang, *Flavor SU(3) Topological Diagram and Irreducible Representation Amplitudes for Heavy Meson Charmless Hadronic Decays: Mismatch and Equivalence*, *Chin. Phys. C* **42** (2018) 103108 [[1803.04227](#)].
- [37] Y. Grossman and S. Schacht, *U-Spin Sum Rules for CP Asymmetries of Three-Body Charmed Baryon Decays*, *Phys. Rev. D* **99** (2019) 033005 [[1811.11188](#)].
- [38] Y. Grossman and S. Schacht, *The emergence of the $\Delta U = 0$ rule in charm physics*, *JHEP* **07** (2019) 020 [[1903.10952](#)].

- [39] H.-Y. Cheng and C.-W. Chiang, *Revisiting CP violation in $D \rightarrow PP$ and VP decays*, *Phys. Rev. D* **100** (2019) 093002 [[1909.03063](#)].
- [40] A. Dery, Y. Grossman, S. Schacht and A. Soffer, *Probing the $\Delta U = 0$ rule in three body charm decays*, *JHEP* **05** (2021) 179 [[2101.02560](#)].
- [41] B. Bhattacharya, A. Datta, A.A. Petrov and J. Waite, *Flavor $SU(3)$ in Cabibbo-favored D -meson decays*, *JHEP* **10** (2021) 024 [[2107.13564](#)].
- [42] S. Schacht, *A U -spin anomaly in charm CP violation*, *JHEP* **03** (2023) 205 [[2207.08539](#)].
- [43] M. Gavrilova, Y. Grossman and S. Schacht, *The mathematical structure of U -spin amplitude sum rules*, *JHEP* **08** (2022) 278 [[2205.12975](#)].
- [44] M. Gavrilova, Y. Grossman and S. Schacht, *Determination of the $D \rightarrow \pi\pi$ ratio of penguin over tree diagrams*, *Phys. Rev. D* **109** (2024) 033011 [[2312.10140](#)].
- [45] M. Gavrilova and S. Schacht, *Systematics of U -Spin Sum Rules for Systems with Direct Sums*, [2409.03830](#).
- [46] S. Iguro, U. Nierste, E. Overduin and M. Schücker, *$SU(3)_F$ sum rules for CP asymmetry of $D_{(s)}$ decays*, [2408.03227](#).
- [47] Y. Grossman, A.L. Kagan and Y. Nir, *New physics and CP violation in singly Cabibbo suppressed D decays*, *Phys. Rev. D* **75** (2007) 036008 [[hep-ph/0609178](#)].
- [48] A. Dery and Y. Nir, *Implications of the LHCb discovery of CP violation in charm decays*, *JHEP* **12** (2019) 104 [[1909.11242](#)].
- [49] R. Bause, H. Gisbert, G. Hiller, T. Höhne, D.F. Litim and T. Steudtner, *U -spin-CP anomaly in charm*, *Phys. Rev. D* **108** (2023) 035005 [[2210.16330](#)].
- [50] H. Leutwyler, *On the $1/N$ expansion in chiral perturbation theory*, *Nucl. Phys. B Proc. Suppl.* **64** (1998) 223 [[hep-ph/9709408](#)].
- [51] T. Feldmann, P. Kroll and B. Stech, *Mixing and decay constants of pseudoscalar mesons*, *Phys. Rev. D* **58** (1998) 114006 [[hep-ph/9802409](#)].
- [52] P. Bickert, P. Masjuan and S. Scherer, *η - η' Mixing in Large- N_c Chiral Perturbation Theory*, *Phys. Rev. D* **95** (2017) 054023 [[1612.05473](#)].
- [53] T. Feldmann, P. Kroll and B. Stech, *Mixing and decay constants of pseudoscalar mesons: The Sequel*, *Phys. Lett. B* **449** (1999) 339 [[hep-ph/9812269](#)].
- [54] L. Gan, B. Kubis, E. Passemar and S. Tulin, *Precision tests of fundamental physics with η and η' mesons*, *Phys. Rept.* **945** (2022) 1 [[2007.00664](#)].
- [55] RQCD collaboration, *Masses and decay constants of the η and η' mesons from lattice QCD*, *JHEP* **08** (2021) 137 [[2106.05398](#)].
- [56] M. Gronau, O.F. Hernandez, D. London and J.L. Rosner, *Broken $SU(3)$ symmetry in two-body B decays*, *Phys. Rev. D* **52** (1995) 6356 [[hep-ph/9504326](#)].
- [57] FLAVOUR LATTICE AVERAGING GROUP (FLAG) collaboration, *FLAG Review 2021*, *Eur. Phys. J. C* **82** (2022) 869 [[2111.09849](#)].
- [58] PARTICLE DATA GROUP collaboration, *Review of particle physics*, *Phys. Rev. D* **110** (2024) 030001.

- [59] D. Kraft, *A Software Package for Sequential Quadratic Programming*, Deutsche Forschungs- und Versuchsanstalt für Luft- und Raumfahrt Köln: Forschungsbericht, Wiss. Berichtswesen d. DFVLR (1988).
- [60] P. Virtanen, R. Gommers, T.E. Oliphant, M. Haberland, T. Reddy, D. Cournapeau et al., *SciPy 1.0: Fundamental Algorithms for Scientific Computing in Python*, *Nature Methods* **17** (2020) 261.
- [61] Bolognani, Carolina, and Nierste, Ulrich and Schacht, Stefan, and Vos, K. Keri, “in progress.”.
- [62] M. Gronau, O.F. Hernandez, D. London and J.L. Rosner, *Decays of B mesons to two light pseudoscalars*, *Phys. Rev. D* **50** (1994) 4529 [[hep-ph/9404283](#)].
- [63] M. Karliner and H.J. Lipkin, *About a Possible Nonstrange Cousin of the Theta+ Pentaquark*, in *Narrow Nucleon Resonances: Predictions, Evidences, Perspectives*, 2, 2010 [[1002.4149](#)].
- [64] D. Sahoo, R. Sinha and N.G. Deshpande, *Model independent method for a quantitative estimation of SU(3) flavor symmetry breaking using Dalitz plot distributions*, *Phys. Rev. D* **91** (2015) 076013 [[1502.07089](#)].
- [65] L. Meng, B. Wang, G.-J. Wang and S.-L. Zhu, *Chiral perturbation theory for heavy hadrons and chiral effective field theory for heavy hadronic molecules*, *Phys. Rept.* **1019** (2023) 1 [[2204.08716](#)].
- [66] T.D. Lee and C.-N. Yang, *Charge Conjugation, a New Quantum Number G, and Selection Rules Concerning a Nucleon Anti-nucleon System*, *Nuovo Cim.* **10** (1956) 749.